Electronic Supplementary Material (ESI) for Dalton Transactions.

Pre- and post-synthetic modulation of the ordering temperatures in a family of anilato-based magnets

Cristian Martínez Hernández, Patricia Gómez-Claramunt, Samia Benmansour* and Carlos J. Gómez-García*

Departamento de Química Inoránica. Instituto de Ciencia Molecular (ICMol). Universidad de Valencia. C/ Catedrático José Beltrán, 2. 46980 Paterna (Valencia), Spain

Supporting information

X-ray powder diffraction

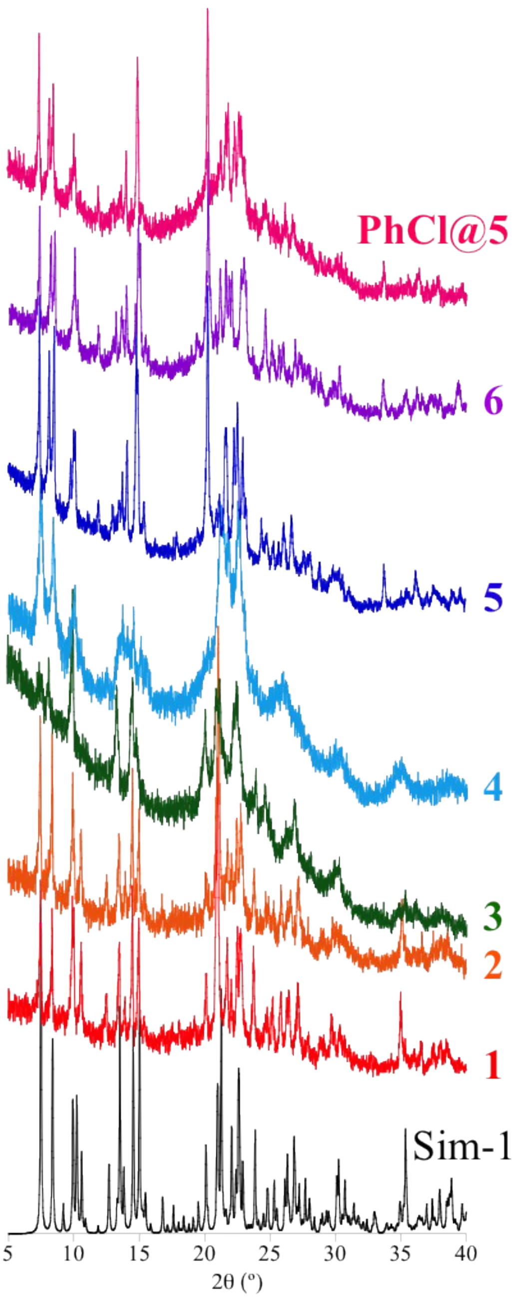

Figure S1. *Experimental X-ray powder difractograms of compounds $(NBu_4)[MnCr(C_6O_4Br_2)_3]\cdot 1.75C_6H_5Br$ (**1**), $(NBu_4)[MnCr(C_6O_4Br_2)_3]\cdot C_6H_5Cl$ (**2**), $(NBu_4)[MnCr(C_6O_4Br_2)_3]\cdot C_6H_5I$ (**3**), $(NBu_4)[MnCr(C_6O_4Br_2)_3]\cdot C_6H_5CH_3$ (**4**), $(NBu_4)[MnCr(C_6O_4Br_2)_3]\cdot 2C_6H_5CN$ (**5**), $(NBu_4)[MnCr(C_6O_4Br_2)_3]\cdot 2C_6H_5NO_2$ (**6**), $(NBu_4)[MnCr(C_6O_4Br_2)_3]\cdot 2C_6H_5CN$ exchanged with C_6H_5Cl (**PhCl@5**) and the simulated one from the single crystal X-ray structure of compound **1**.*

Table S1. Unit cell parameters of compounds $(NBu_4)[MnCr(C_6O_4Br_2)_3]\cdot 1.75C_6H_5Br$ (**1**), $(NBu_4)[MnCr(C_6O_4Br_2)_3]\cdot C_6H_5Cl$ (**2**), $(NBu_4)[MnCr(C_6O_4Br_2)_3]\cdot C_6H_5I$ (**3**), $(NBu_4)[MnCr(C_6O_4Br_2)_3]\cdot C_6H_5CH_3$ (**4**), $(NBu_4)[MnCr(C_6O_4Br_2)_3]\cdot 2C_6H_5CN$ (**5**), $(NBu_4)[MnCr(C_6O_4Br_2)_3]\cdot 2C_6H_5NO_2$ (**6**) and $(NBu_4)[MnCr(C_6O_4Br_2)_3]\cdot 2C_6H_5CN$ exchanged with C_6H_5Cl (**PhCl@5**) determined from their X-ray powder diffractograms at room temperature.

compound	a (Å)	b (Å)	c (Å)	β (º)	Volume (Å^3)
$(NBu_4)[MnCr(C_6O_4Br_2)_3]\cdot 1.75C_6H_5Br$ (**1**)[a]	9.9557(5)	23.6054(10)	12.2129(6)	105.187(5)	2769.9(2)
$(NBu_4)[MnCr(C_6O_4Br_2)_3]\cdot 1.75C_6H_5Br$ (**1**)[b]	10.104(4)	23.70(1)	12.363(5)	106.78(4)	2834.17
$(NBu_4)[MnCr(C_6O_4Br_2)_3]\cdot C_6H_5Cl$ (**2**)	10.049(4)	23.69(1)	12.330(6)	106.85(4)	2809.36
$(NBu_4)[MnCr(C_6O_4Br_2)_3]\cdot C_6H_5I$ (**3**)	9.92(2)	23.59(9)	12.50(5)	106.2(3)	2807.14
$(NBu_4)[MnCr(C_6O_4Br_2)_3]\cdot C_6H_5CH_3$ (**4**)	9.98(2)	23.64(7)	12.19(3)	105.9(3)	2768.64
$(NBu_4)[MnCr(C_6O_4Br_2)_3]\cdot 2C_6H_5CN$ (**5**)	9.88(2)	23.36(9)	12.25(4)	105.7(3)	2720.91
$(NBu_4)[MnCr(C_6O_4Br_2)_3]\cdot 2C_6H_5NO_2$ (**6**)	9.81(3)	23.4(1)	12.15(6)	106.3(5)	2834.17
$(NBu_4)[MnCr(C_6O_4Br_2)_3]\cdot C_6H_5Cl$ (**PhCl@5**)	9.91(1)	23.38(5)	12.21(2)	105.6(2)	2727.00

[a] Single crystal X-ray data at 120 K.
[b] Determined from X-ray powder data at room temperature

IR spectroscopy

Table S2. Selected vibrational frequencies (cm^{-1}) for compounds $(NBu_4)[MnCr(C_6O_4Br_2)_3]\cdot 1.75C_6H_5Br$ (**1**), $(NBu_4)[MnCr(C_6O_4Br_2)_3]\cdot C_6H_5Cl$ (**2**), $(NBu_4)[MnCr(C_6O_4Br_2)_3]\cdot C_6H_5I$ (**3**), $(NBu_4)[MnCr(C_6O_4Br_2)_3]\cdot C_6H_5CH_3$ (**4**), $(NBu_4)[MnCr(C_6O_4Br_2)_3]\cdot 2C_6H_5CN$ (**5**), $(NBu_4)[MnCr(C_6O_4Br_2)_3]\cdot 2C_6H_5NO_2$ (**6**), $(NBu_4)[MnCr(C_6O_4Br_2)_3]\cdot 2C_6H_5CN$ exchanged with C_6H_5Cl (**PhCl@5**) and $(NBu_4)[MnCr(C_6O_4Br_2)_3]$ (**7**).

Band	PhBr (**1**)	PhCl (**2**)	PhI (**3**)	$PhCH_3$ (**4**)	PhCN (**5**)	$PhNO_2$ (**6**)	PhCl (**PhCl@5**)	- (**7**)
ν(C-H)	2958 2935 2878	2959 2930 2880	2959 2928 2871	2961 2934 2872	2960 2933 2874	2963 2933 2873	2959 2928 2872	2960 2923 2873
ν(C=O)	1602	1616	1635	1626	1603	1616	1601	1603
ν(C=C) + ν(C-O)	1489	1490	1492	1490	1490	1490	1486	1490
δ(C-H)	1382	1384	1384	1383	1383	1384	1382	1385
ν(C-C) + ν(C-O)	1353	1353	1356	1353	1355	1350	1353	1356
δ(C-Br)	818	817	820	819	817	819	818	817
ρ(C-Br)	562	562	560	561	562	562	562	560
ν(C=C)[1]	1508*	1505	1508	1505	1506	1506	1505	1506
δ(C-H)[1]	686 736	685 740	685 731	686 733	694 730	683 705	685 740	-
ν(CN)[1]	-	-	-	2226	-	-	-	-
$\nu(N\text{-}O)_{as}$[1]	-	-	-	-	-	1520	-	-
$\nu(N\text{-}O)_{s}$[1]	-	-	-	-	-	1343	-	-
ν(C-N)[1]	-	-	-	-	-	875	-	-

1- Solvent bands; *shoulder.

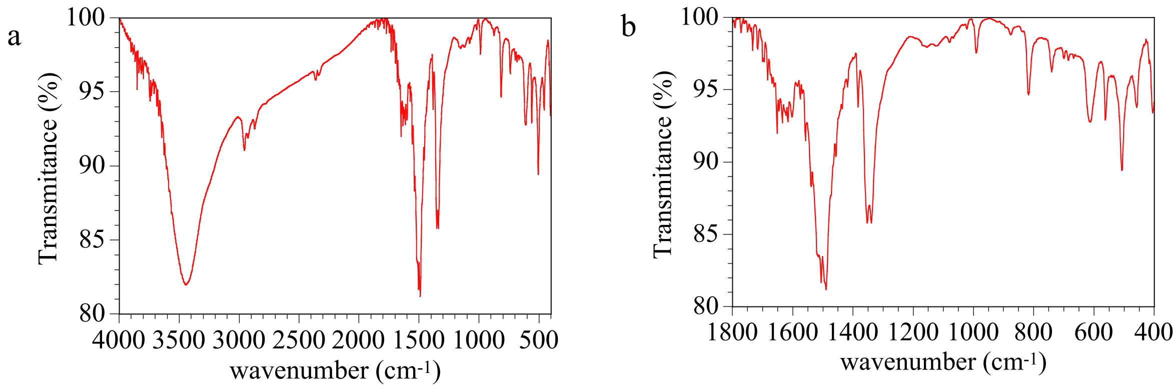

Figure S2. *FT-IR spectra of compound* ***1*** *in* ***(a)*** *the 4000-400 cm*$^{-1}$ *region and* ***(b)*** *the 1800-400 cm*$^{-1}$ *region.*

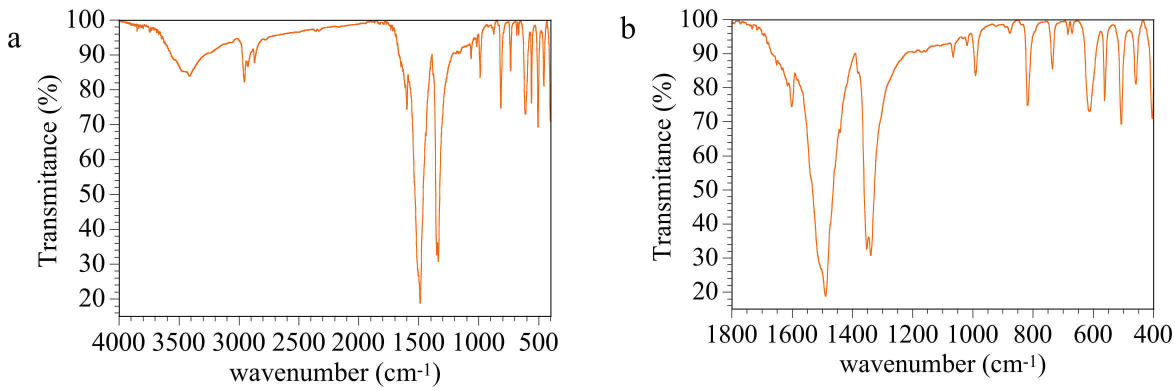

Figure S3. *FT-IR spectra of compound* ***2*** *in* ***(a)*** *the 4000-400 cm*$^{-1}$ *region and* ***(b)*** *the 1800-400 cm*$^{-1}$ *region.*

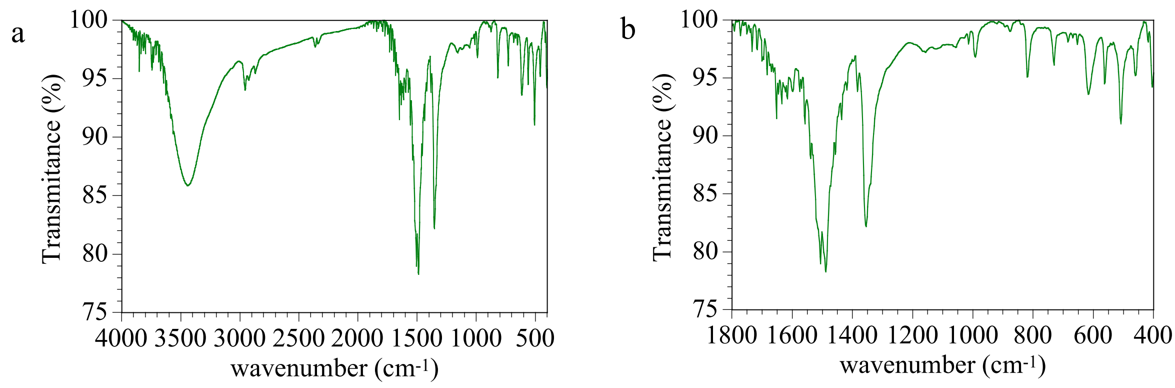

Figure S4. *FT-IR spectra of compound* ***3*** *in* ***(a)*** *the 4000-400 cm*$^{-1}$ *region and* ***(b)*** *the 1800-400 cm*$^{-1}$ *region.*

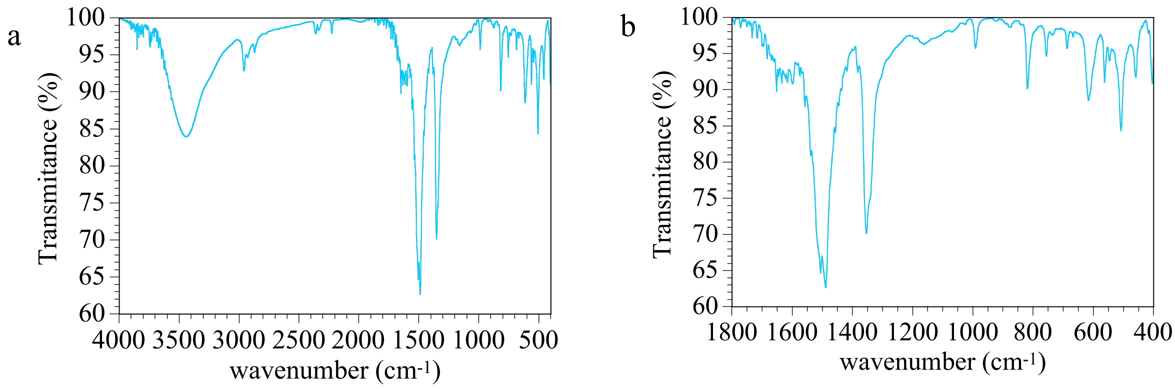

Figure S5. *FT-IR spectra of compound **4** in **(a)** the 4000-400 cm^{-1} region and **(b)** the 1800-400 cm^{-1} region.*

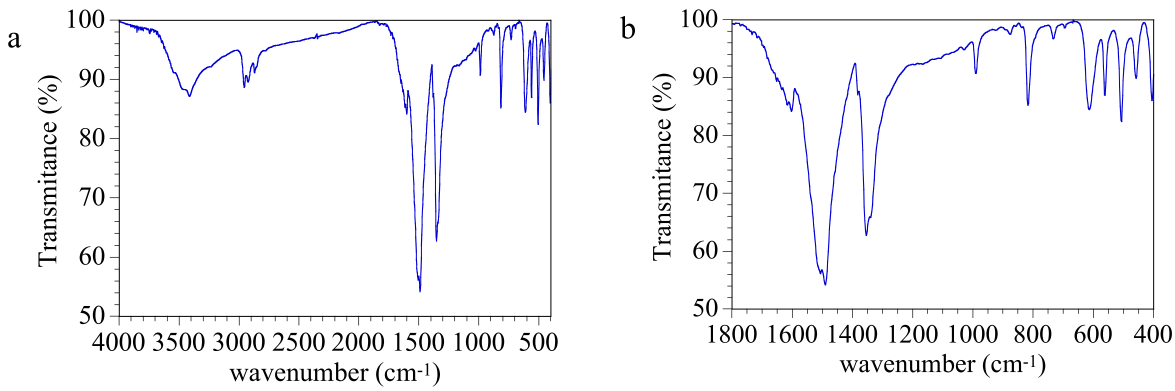

Figure S6. *FT-IR spectra of compound **5** in **(a)** the 4000-400 cm^{-1} region and **(b)** the 1800-400 cm^{-1} region.*

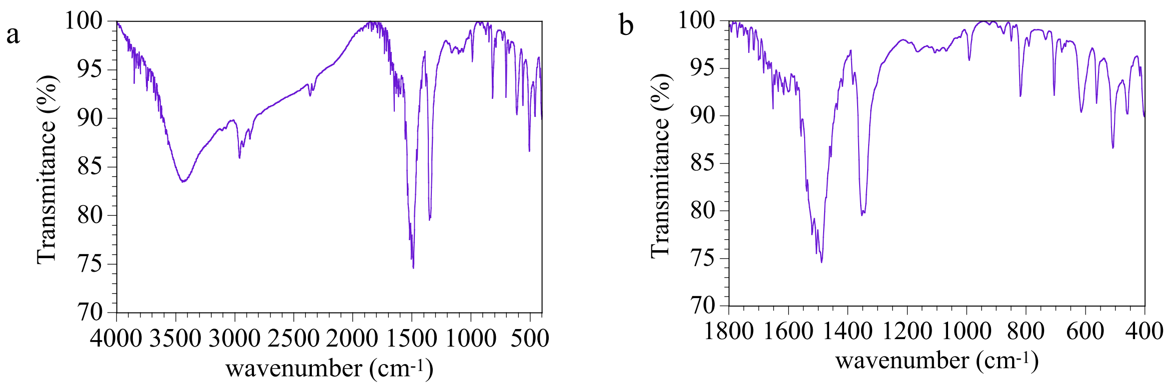

Figure S7. *FT-IR spectra of compound **6** in **(a)** the 4000-400 cm^{-1} region and **(b)** the 1800-400 cm^{-1} region.*

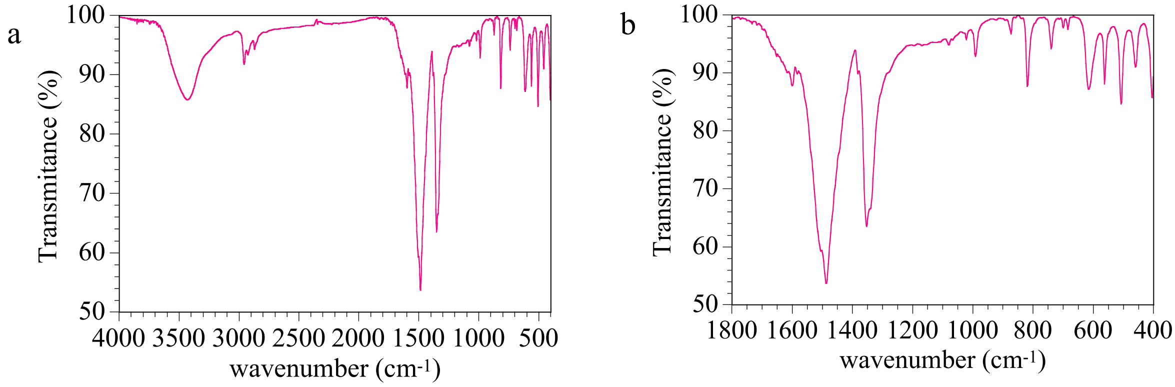

Figure S8. *FT-IR spectra of compound* ***PhCl@5*** *in* ***(a)*** *the 4000-400 cm^{-1} region and* ***(b)*** *the 1800-400 cm^{-1} region.*

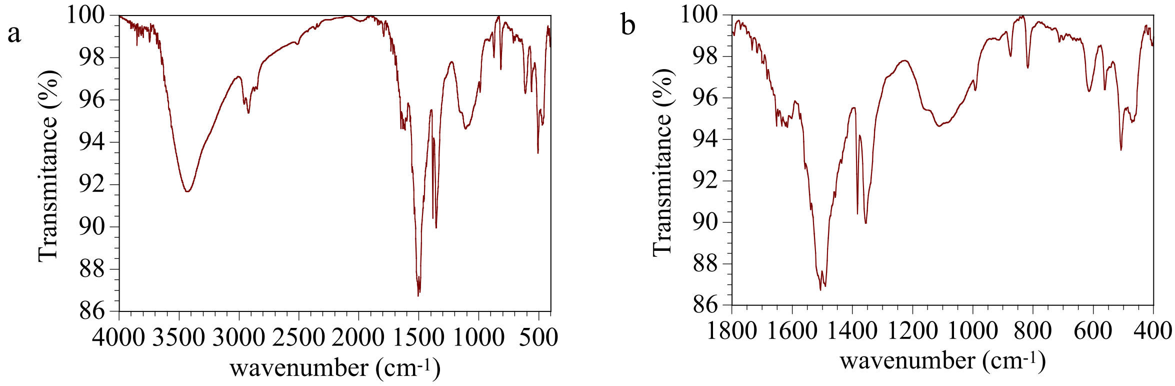

Figure S9. *FT-IR spectra of compound 7 in* ***(a)*** *the 4000-400 cm^{-1} region and* ***(b)*** *the 1800-400 cm^{-1} region.*

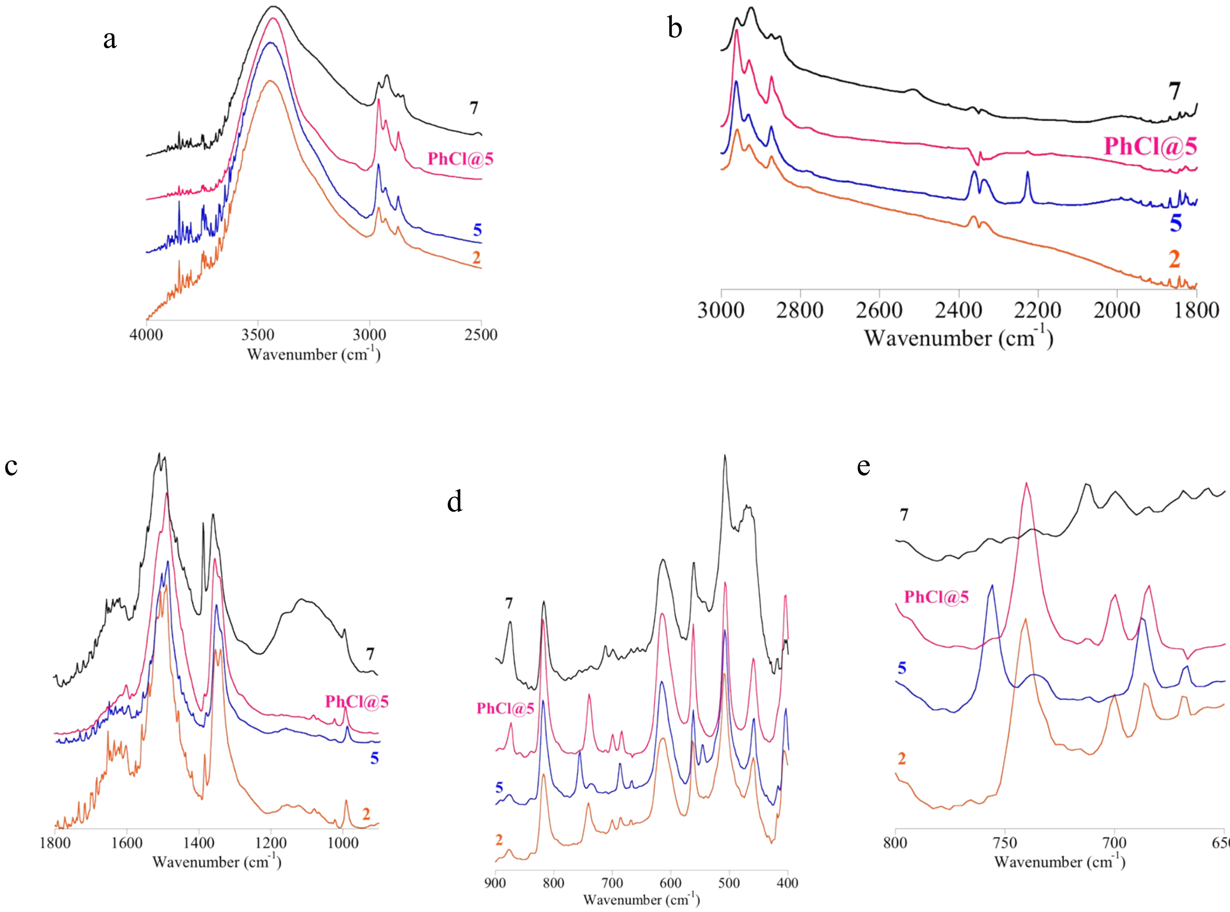

Figure S10. *FT-IR spectra of compounds* ***2***, ***5***, ***PhCl@5*** *and 7 in the* ***(a)*** *the 4000-2500 cm^{-1},* ***(b)*** *the 3000-1800 cm^{-1},* ***(c)*** *the 1800-900 cm^{-1},* ***(d)*** *the 900-400 cm^{-1} and* ***(e)*** *the 800-400 cm^{-1} regions.*

Thermogravimetric analysis

Table S3. Weight loss and the corresponding solvent molecules in compounds $(NBu_4)[MnCr(C_6O_4Br_2)_3]\cdot 1.75C_6H_5Br$ (**1**), $(NBu_4)[MnCr(C_6O_4Br_2)_3]\cdot C_6H_5Cl$ (**2**), $(NBu_4)[MnCr(C_6O_4Br_2)_3]\cdot C_6H_5I$ (**3**), $(NBu_4)[MnCr(C_6O_4Br_2)_3]\cdot C_6H_5CH_3$ (**4**), $(NBu_4)[MnCr(C_6O_4Br_2)_3]\cdot 2C_6H_5CN$ (**5**) and $(NBu_4)[MnCr(C_6O_4Br_2)_3]\cdot 2C_6H_5NO_2$ (**6**).

Compound	**temperature range (ºC)**	**Experimental weight loss (%)**	**solvent**	**Calculated weight loss (%)**
1	30-280	18.1	$1.75C_6H_5Br$	18.2
2	30-190	7.8	C_6H_5Cl	8.3
3	30-270	11.4	C_6H_5I	14.1
4	30-190	6.9	$C_6H_5CH_3$	6.9
5	30-190	13.2	$2\ C_6H_5CN$	14.3
6	30-270	14.5	$2\ C_6H_5NO_2$	16.6
PhCl@5	30-190	10.5	C_6H_5Cl	8.3

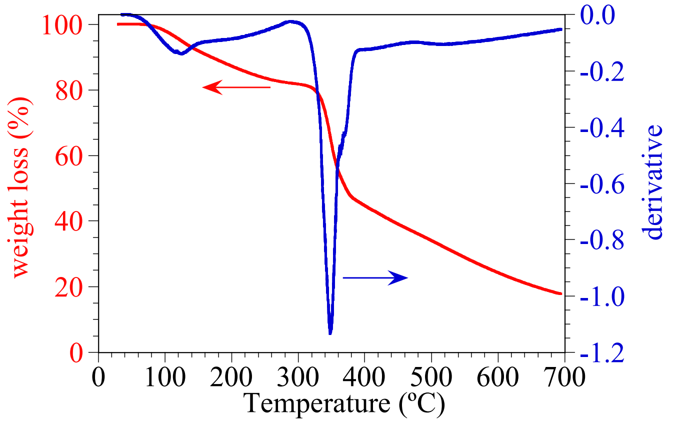

***Figure S11**. Thermogravimetric measurements of $(NBu_4)[MnCr(C_6O_4Br_2)_3]\cdot 1.75C_6H_5Br$ (**1**).*

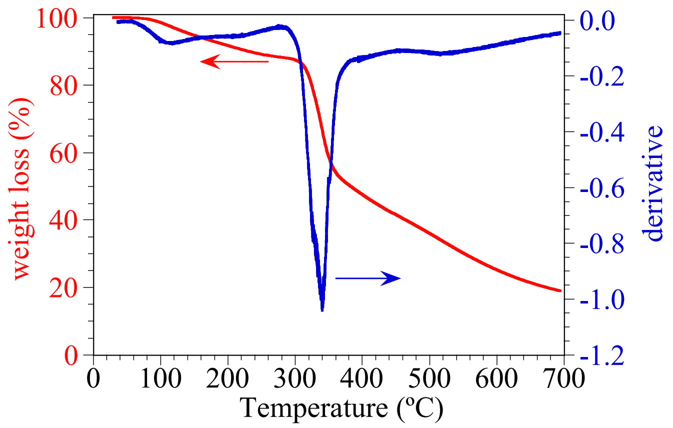

***Figure S12**. Thermogravimetric measurements of $(NBu_4)[MnCr(C_6O_4Br_2)_3]\cdot C_6H_5Cl$ (**2**).*

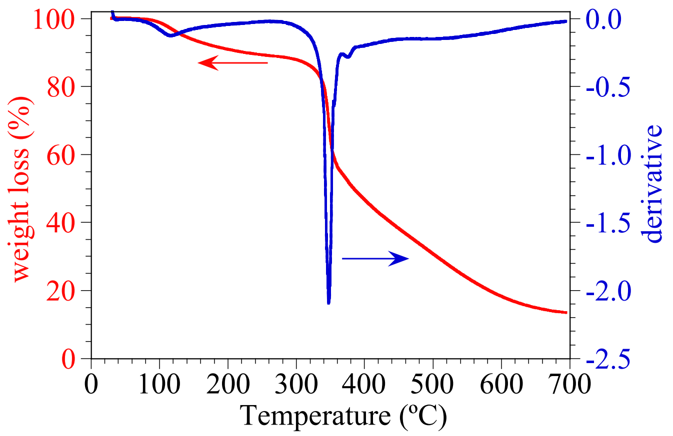

Figure S13. *Thermogravimetric measurements of (NBu$_4$)[MnCr(C$_6$O$_4$Br$_2$)$_3$]·C$_6$H$_5$I (**3**).*

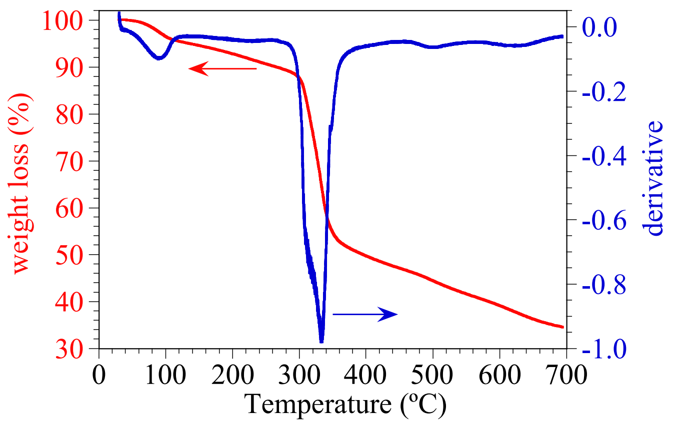

Figure S14. *Thermogravimetric measurements of (NBu$_4$)[MnCr(C$_6$O$_4$Br$_2$)$_3$]·C$_6$H$_5$CH$_3$ (**4**).*

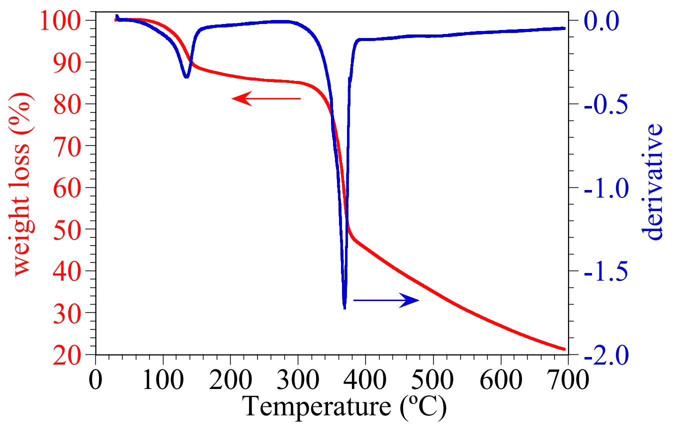

Figure S15. *Thermogravimetric measurements of (NBu$_4$)[MnCr(C$_6$O$_4$Br$_2$)$_3$]·2C$_6$H$_5$CN (**5**).*

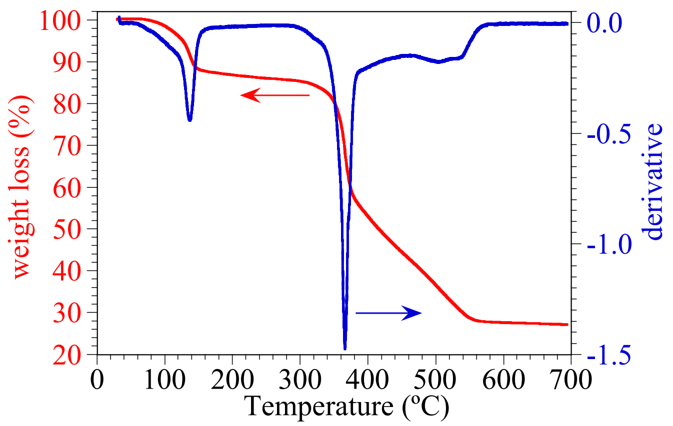

Figure S16*. Thermogravimetric measurements of (NBu$_4$)[MnCr(C$_6$O$_4$Br$_2$)$_3$]·2C$_6$H$_5$NO$_2$ (**6**).*

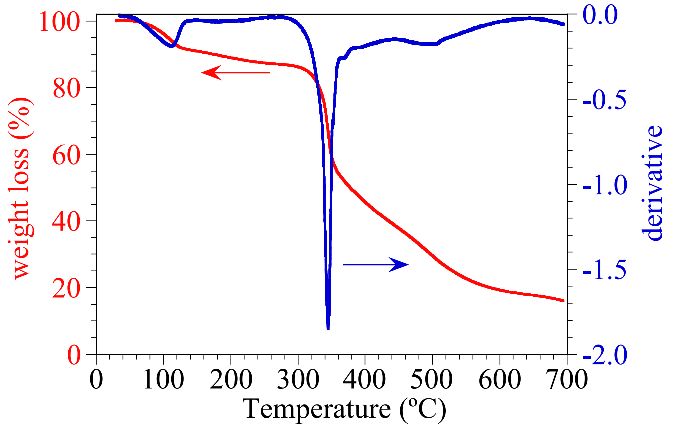

Figure S17*. Thermogravimetric measurements of (NBu$_4$)[MnCr(C$_6$O$_4$Br$_2$)$_3$]·2C$_6$H$_5$CN exchanged with C$_6$H$_5$Cl (**PhCl@5**).*

Table S4. Average Mn-O and Cr-O bond distances (Å) in all the reported bromanilato-bridged Mn(II)Cr(III) compounds.

CCDC	A^+	Mn-O (a)	Cr-O (b)	T_c (K)	Ref.
MIRFIE	$(H_3O)(phz)_3^+$	2.102(15)[a]	2.102(15)[a]	6.0	1
HOWHIM	Fe(sal$_2$-epe)$^+$	2.030(18)[a]	2.030(18)[a]	10.2	2
HOWHOS	Fe(5-Cl-sal$_2$-trien)$^+$	2.16(3)	1.980(15)	9.8	2
MUMLAJ	[Fe(acac$_2$-trien)]$^+$	2.16(3)	1.980(6)	11.1	3
MUMLEN	[Ga(acac$_2$-trien)]$^+$	2.180(4)	1.976(5)	11.6	3
SEPLAD	$Me_2NH_2^+$	2.208(12)	1.972(9)	7.9	4
SEPLEH	$Et_2NH_2^+$	2.171(16)	1.962(13)	8.9	4
SEPROX	Et(i-Pr)$_2$NH$^+$	2.17(2)	1.985(18)	9.0	4
1	NBu_4^+	2.14(3)	1.98(2)	9.5	this work

[a]Mn and Cr atoms are crystallografically equivalent.

Magnetic Properties

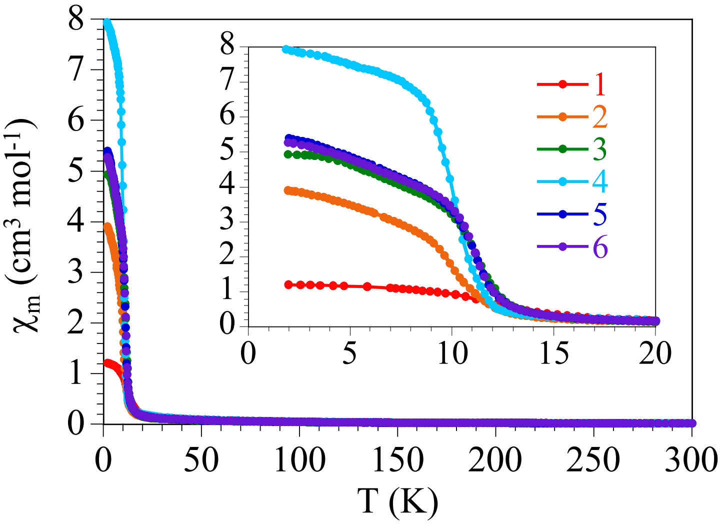

Figure S18. *Thermal variation of χ_m for compounds **1-6**. Inset shows the low temperature region.*

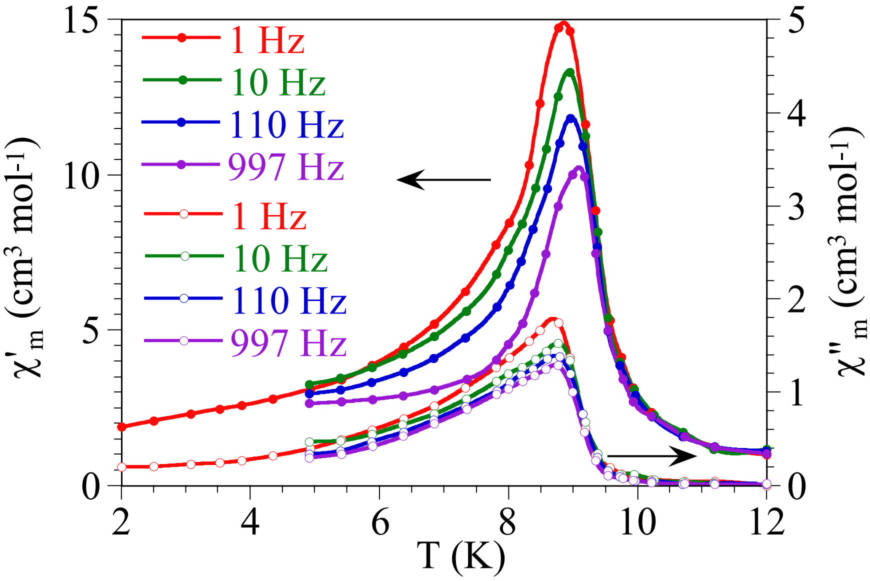

Figure S19. *Thermal variation of the in phase (χ', filled circles, left scale) and out of phase (χ", empty circles, right scale) AC susceptibility at different frequencies for compound $(NBu_4)[MnCr(C_6O_4Br_2)_3]\cdot 1.75C_6H_5Br$ (**1**)*

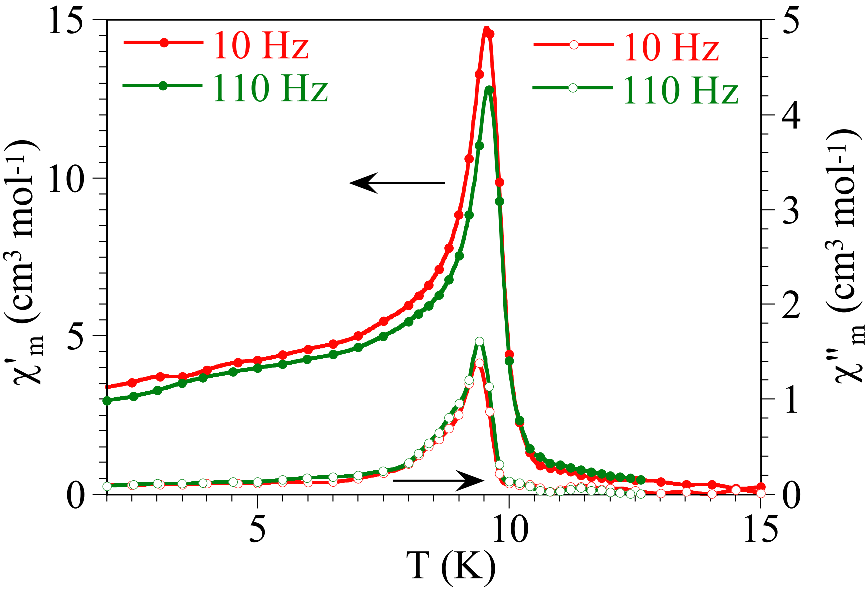

Figure S20. *Thermal variation of the in phase (χ', filled circles, left scale) and out of phase (χ", empty circles, right scale) AC susceptibility at different frequencies for compound* $(NBu_4)[MnCr(C_6O_4Br_2)_3)]\cdot C_6H_5Cl$ *(**2**)*

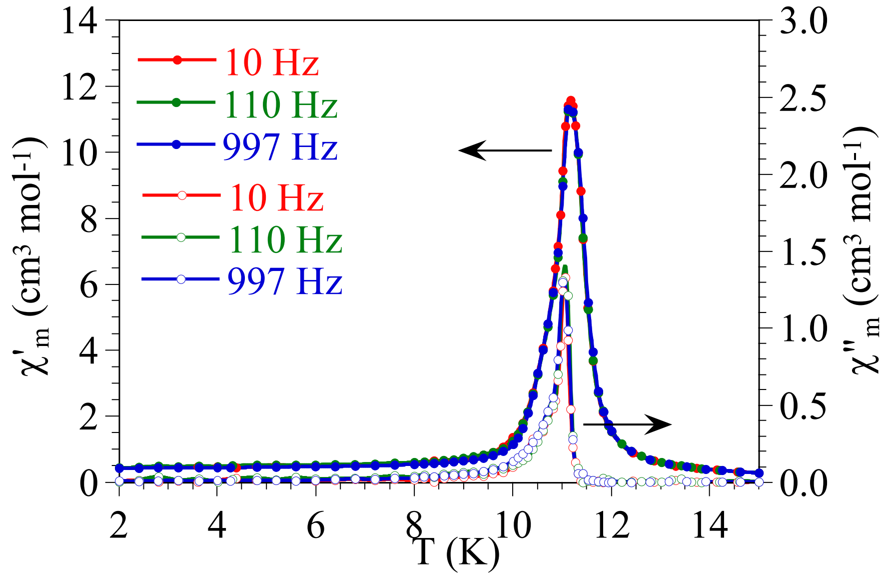

Figure S21. *Thermal variation of the in phase (χ', filled circles, left scale) and out of phase (χ", empty circles, right scale) AC susceptibility at different frequencies for compound* $(NBu_4)[MnCr(C_6O_4Br_2)_3)]\cdot C_6H_5I$ *(**3**)*

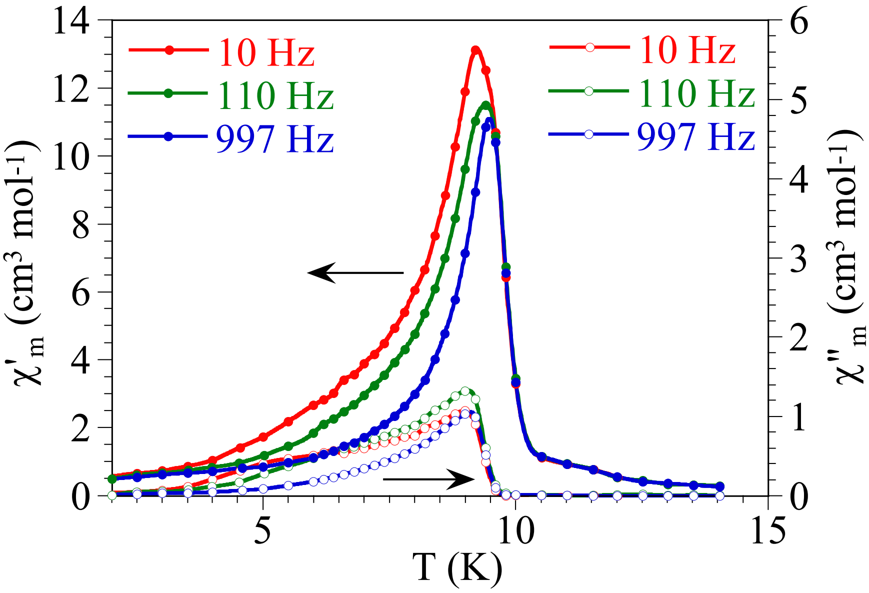

Figure S22. *Thermal variation of the in phase (χ', filled circles, left scale) and out of phase (χ'', empty circles, right scale) AC susceptibility at different frequencies for compound* *$(NBu_4)[MnCr(C_6O_4Br_2)_3)]\cdot C_6H_5CH_3$* ***(4)***

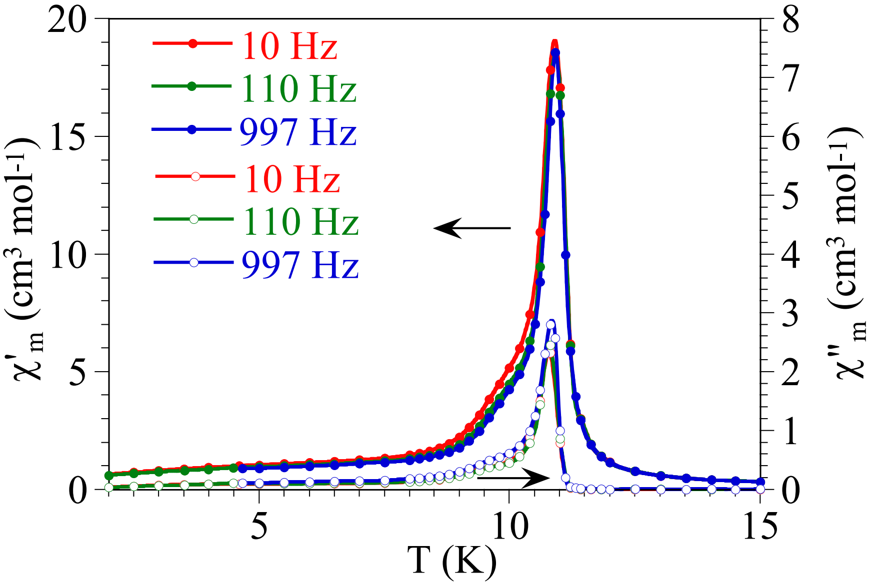

Figure S23. *Thermal variation of the in phase (χ', filled circles, left scale) and out of phase (χ'', empty circles, right scale) AC susceptibility at different frequencies for compound* *$(NBu_4)[MnCr(C_6O_4Br_2)_3)]\cdot 2C_6H_5CN$* ***(5)***

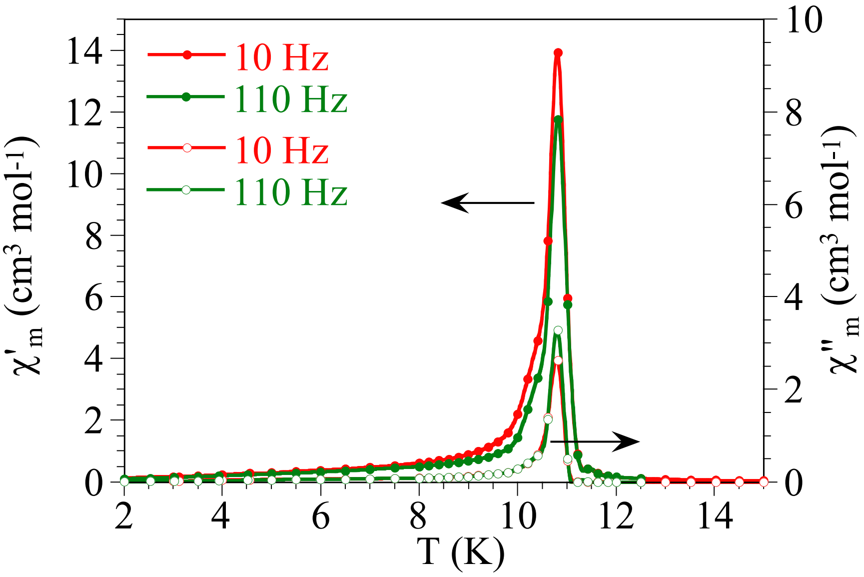

Figure S24. *Thermal variation of the in phase (χ', filled circles, left scale) and out of phase (χ'', empty circles, right scale) AC susceptibility at different frequencies for compound* *$(NBu_4)[MnCr(C_6O_4Br_2)_3)]·2C_6H_5NO_2$* ***(6)***

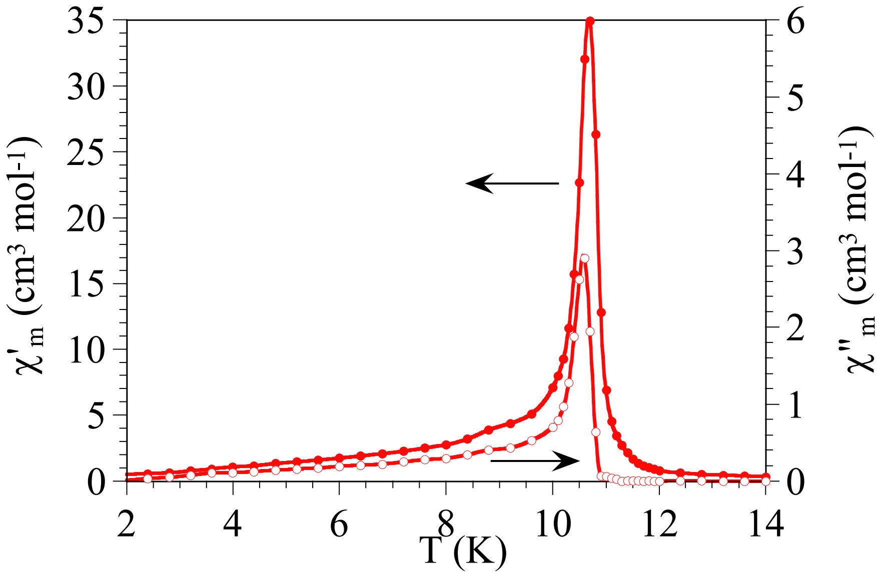

Figure S25. *Thermal variation of the in phase (χ', filled circles, left scale) and out of phase (χ'', empty circles, right scale) AC susceptibility at 110 Hz for compound* ***PhCl@5***.

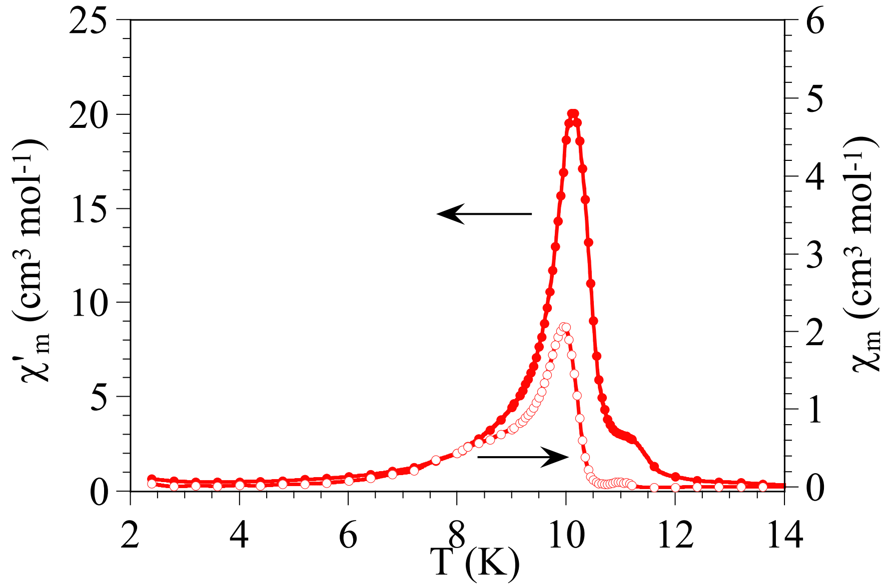

Figure S26*. Thermal variation of the in phase (χ', filled circles, left scale) and out of phase (χ", empty circles, right scale) AC susceptibility at 110 Hz for compound* ***PhCl@5*** *after heating at 400 K (7).*

References

1. Atzori, M.; Benmansour, S.; Mínguez Espallargas, G.; Clemente-León, M.; Abhervé, A.; Gómez-Claramunt, P.; Coronado, E.; Artizzu, F.; Sessini, E.; Deplano, P.; Serpe, A.; Mercuri, M. L.; Gómez García, C. J. A Family of Layered Chiral Porous Magnets Exhibiting Tunable Ordering Temperatures. *Inorg. Chem.* **2013***, 52*, 10031-10040.

2. Abhervé, A.; Clemente-León, M.; Coronado, E.; Gómez-García, C. J.; Verneret, M. One-Dimensional and Two-Dimensional Anilate-Based Magnets with Inserted Spin-Crossover Complexes. *Inorg. Chem.* **2014***, 53*, 12014-12026.

3. Abhervé, A.; Mañas-Valero, S.; Clemente-León, M.; Coronado, E. Graphene related magnetic materials: micromechanical exfoliation of 2D layered magnets based on bimetallic anilate complexes with inserted $[Fe^{III}(acac_2\text{-trien})]^+$ and $[Fe^{III}(sal_2\text{-trien})]^+$ molecules. *Chem. Sci.* **2015***, 6*, 4665-4673.

4. Palacios-Corella, M.; Fernández-Espejo, A.; Bazaga-García, M.; Losilla, E. R.; Cabeza, A.; Clemente-León, M.; Coronado, E. Influence of Proton Conducting Cations on the Structure and Properties of 2D Anilate-Based Magnets. *Inorg. Chem.* **2017***, 56*, 13865-13877.